Available online at www.sciencedirect.com
ScienceDirect
International Journal of Heat and Mass Transfer 50 (2007) 3658–3669
International Journal of HEAT and MASS TRANSFER
www.elsevier.com/locate/ijhmt

Mass diffusion through two-layer porous media: an application to the drug-eluting stent

Giuseppe Pontrelli [a,*], Filippo de Monte [b]

[a] Istituto per le Applicazioni del Calcolo – CNR, Viale del Policlinico, 137 – 00161 Roma, Italy
[b] Dipartimento di Ingegneria Meccanica, Energetica e Gestionale, University of L'Aquila, Località Monteluco, 67040 Roio Poggio (AQ), Italy

Received 2 June 2006
Available online 2 January 2007

Abstract

A mathematical model for the diffusion–transport of a substance between two porous homogeneous media of different properties and dimensions is presented. A strong analogy with the one-dimensional transient heat conduction process across two-layered slabs is shown and a similar methodology of solution is proposed. Separation of variables leads to a Sturm–Liouville problem with discontinuous coefficients and an exact analytical solution is given in the form of an infinite series expansion. The model points out the role of four non-dimensional parameters which control the diffusion mechanism across the two porous layers. The drug-eluting stent constitutes the main application of the present model. Drug concentration profiles at various times are given and analyzed. Also, qualitative considerations and a quantitative description to evaluate feasibility of new drug delivery strategies are provided, and some indicators, such as the emptying time, useful to optimize the drug-eluting stent design are discussed.

Keywords: Mass diffusion; Multi-layered porous media; Advection–diffusion equation; Sturm–Liouville problem; Drug delivery; Pharmacokinetics

1. Introduction

In last years, polymeric gels are widely used as drug carriers devices in many biotechnological applications, such as tissue engineering [1]. A matrix of gel is filled with a specific drug which is subsequently released into the living tissue. To have a desired therapeutic effect, the concentration of the drug in the tissue should lie within a given range. If below that, the therapy results ineffective. On the other hand, if the concentration is above a threshold value, the drug can produce a toxic effect [2].

A recent clinical application of such a technology are the drug-eluting stents: these are complex medical devices inserted in the arterial wall aimed to widen the lumen of stenosed arteries, to prevent occlusion, and to restore the blood flow perfusion to the downstream tissues [2–4] (Fig. 1). Drug-eluting stents combine the mechanical support with local drug delivery to the arterial tissue to fight early restenosis caused by proliferation of smooth muscle cells. To this aim, a polymeric matrix (gel) is added to the metallic struts and loaded with a drug which is released after implantation. The stent struts can be uniformly covered by the polymer (coated stent) or it can contain honeycombed strut elements with an inlaid polymer (stent with drug reservoirs) (Fig. 2) [5]. It is recognized that the time and rate of the drug release is crucial for the therapy. This process is influenced by many factors, such as properties of the drug (hydrophily), coating (structure and material parameters) as well as the transport characteristics of the arterial wall. Although intravascular stents are designed to operate in static regimes, they act under complex stress conditions, varying in time and it is difficult to forecast their performance and efficiency over long times. Mathematical models predicting the dynamics of solute concentration and mass flux

* Corresponding author. Tel.: +39 6 884 70251; fax: +39 6 440 4306.
E-mail addresses: pontrelli@iac.rm.cnr.it (G. Pontrelli), demonte@ing.univaq.it (F. de Monte).

0017-9310/$ - see front matter © 2006 Elsevier Ltd. All rights reserved.
doi:10.1016/j.ijheatmasstransfer.2006.11.003

Nomenclature

c_i	mass volume-averaged concentration in the ith layer
c_i'	fluid-phase concentration in the ith layer
D_i	drug diffusive coefficient in the ith layer
J	mass flux at the interface $x = 0$ (Fig. 3)
k	partition coefficient
L	thickness ratio, $\frac{L_1}{L_2}$.
L_i	thickness of the ith layer
M_i	dimensionless mass per unit of area in the ith layer
P	membrane permeability coefficient
S	concentration jump at the interface $x = 0$ (Fig. 3)
t	time
t_E	emptying time of drug
x	space coordinate
X_i	eigenfunction of the ith layer

Greek symbols

γ	diffusivity ratio, $\frac{D_1}{D_2}$
ϵ	medium porosity
λ_i	eigenvalue of the ith layer
σ	material ratio, $\frac{k_1\epsilon_1}{k_2\epsilon_2}$
ϕ	nondimensional permeability, $\frac{PL_2}{D_2k_2\epsilon_2}$

Subscripts

1	first layer (coating)
2	second layer (wall)

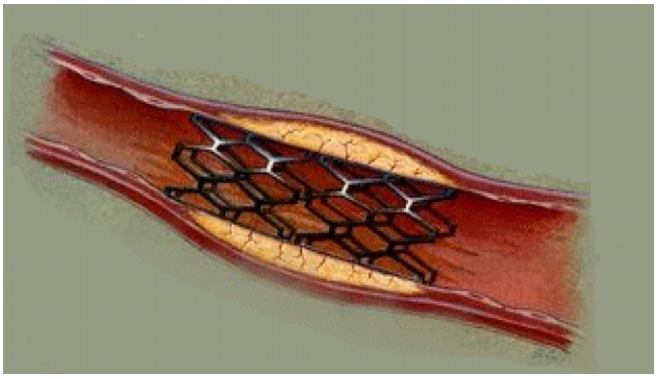

Fig. 1. Sketch of a stented artery.

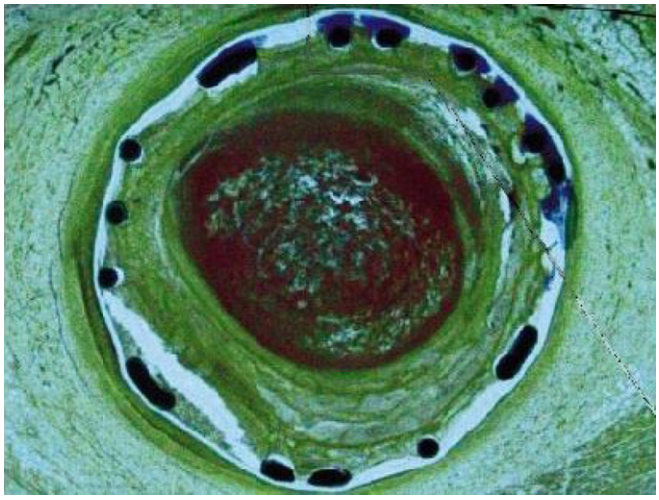

Fig. 2. Section of a stented artery with the struts (in black) embedded into the wall (courtesy of P. Zunino).

are of interest for biomedical engineers and clinicians, as they offer a simple tool for optimizing the drug delivery design and technology.

A number of recent studies has been devoted to the mass transfer process in the arterial wall, modelled as a multi-layered medium, coupled with the transport in the lumen [6,7]. Some work has been done to correlate the number and the location of the metallic net structure of a stent with the extension of the perfused area [8]. Other mathematical models have been developed to predict the release of a substance in a tissue and the influence of the physical properties of the drug. However, computational difficulties in coupling different geometrical scales are reported [5,9].

The present paper provides a fundamental study of the transient mass elution between two homogeneous porous media having different thickness and material properties. The treatment is quite general and can be applied to several mass transfer diffusion dominated problems in composite materials. The main application is the drug-eluting stent, where the whole drug is initially in a polymeric matrix coating the metallic structure and is subsequently released into the arterial wall. Being interested in the pharmacokinetics only, any structural analysis as well as all mechanical effects of the stent are neglected. The chemistry and the binding of the drug to the tissue are beyond the scope of the present work and will not be considered here. An outline of the paper is now given.

Section 2 presents the time–space diffusion–transport equation for the dynamics of a substance across a double layer structured material in the general case. Due to a prevalent flux direction, the problem is written in one dimensional case in terms of nondimensional variables. This results in a coupled system of partial differential equations in two domains with an interface condition. Despite the surprising analogy between mass transfer and heat conduction problems, solutions of identical form are admitted provided that not only the differential equations, but also the initial and boundary conditions match [10]. In the current case, however, the boundary conditions at the

interface do not have a counterpart in the heat diffusion problem. Differently that in the case of two-layer heat conduction, the mass flux is continuous, but a concentration jump may occur at the interface. This follows from the equilibrium conditions with regard to mass transfer (equality of the chemical potential of each component in each phase, see [11, chapter XI]). As a consequence, the solution to the transient two-layer heat conduction problem proposed in [16] cannot entirely be transferred to the analogous mass diffusion process of interest here. However, the same theoretical procedure based on separation of variables for solving the differential problem may be reformulated, as shown in Section 3. Thus the correspondent Sturm–Liouville problem is analyzed and the correspondent eigenvalue equation is solved. Finally, the concentration solution is expressed in the form of a Fourier series (Section 3).

Compared to a fully numerical method, the analytical approach provides a greater insight into the physical sense of the drug delivery process. As a matter of fact, the present one-dimensional model is shown to catch most of the relevant aspects of the drug dynamics. By showing relationships among the relevant variables and material parameters, it can be used to identify simple indexes or clinical indicators of biomechanical significance. Moreover the methodology can be easily extended to a multi-layered coating and wall structure. The model enables the effect of important factors such as drug diffusivity, coating thickness, and membrane permeability to be analyzed. Tuned in optimal way, they can be used to design novel release mechanisms, as well as to improve drug delivery protocols used in therapy and diagnostics.

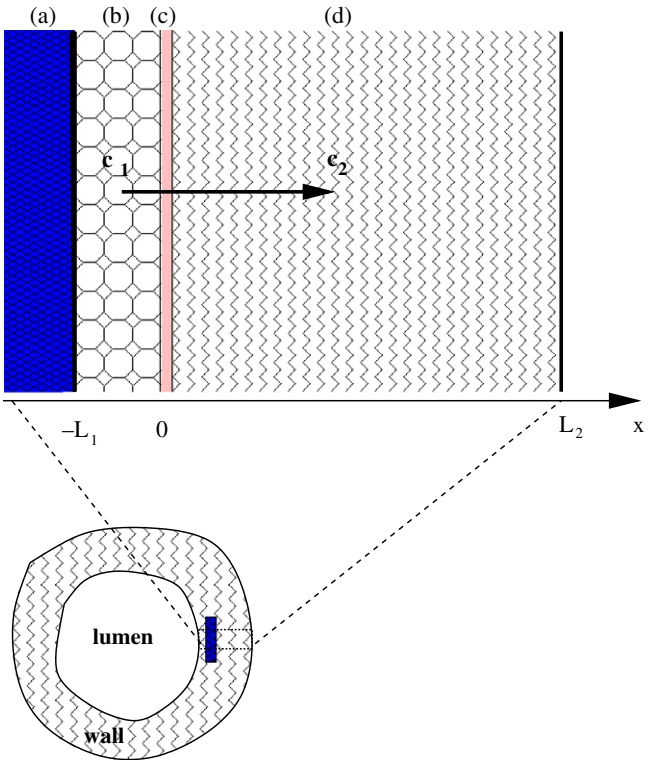

Fig. 3. Cross-section of a stented artery with a zoomed area near the wall that shows the metallic mesh and the two-layer medium at the adventitial side described by the model (2.1) and (2.2): (a) stent strut, (b) coating, (c) topcoat, (d) arterial wall. Due to an initial difference of concentration, drug is diffusing in the arterial wall from (b) to (d) through the permeable membrane (c). An analogous two-layer pattern is present on the opposite side of the strut, referring to the drug diffusion towards the lumen (lumenal side).

2. Formulation of the problem

A drug-eluting stent (DES) is a metallic prosthesis (*strut*) implanted into the arterial wall and coated with a thin layer of biocompatible polymeric gel that encapsulates a therapeutic drug (*coating*). Such a drug, released in a controlled manner through a permeable membrane, is aimed at healing the vascular tissues or at preventing a possible restenosis by virtue of its anti-proliferative action against smooth muscle cells. In the present work we are interested in the mechanism of drug elution into the arterial tissue. As a matter of fact any other effects, such as the drug metabolism in the living tissue and a possible decomposition of the polymeric matrix, are neglected.

Let us consider a stent coated by a thin layer (of thickness L_1) of gel containing a drug and embedded into the arterial wall (of thickness L_2), as illustrated in Fig. 3. The complex multi-layered structure of the arterial wall has been disregarded and a homogeneous material with averaged properties has been considered for simplicity (*fluid-wall* model) as in Refs. [9,13]. Both the coating and the arterial wall are treated as porous media [14]. Because most of the mass transport process occurs along the direction normal to the two layers (radial direction), we restrict our study to a simplified 1D model. In particular, we consider a radial line crossing the metallic strut, the coating and the arterial wall and pointing outwards and, being the wall thickness very small with respect to the arterial radius, a Cartesian coordinate system x is used along it (Fig. 3).

At the initial time ($t = 0$), the drug is contained only in the coating and it is uniformly distributed at a maximum concentration C_1 and, subsequently, it is released into the wall. Here, and throughout this paper, a mass volume-averaged concentration $c(x,t)$ (mg/ml) is considered. Since the strut is impermeable to the drug, no mass flux passes through the boundary surface $x = -L_1$. Moreover, it is assumed that the plasma does not penetrate the surface of the stent. Thus, the dynamics of the drug in the coating (first layer) is described by the following 1D differential equation:

$$\begin{aligned} &\frac{\partial c_1}{\partial t} - D_1 \frac{\partial^2 c_1}{\partial x^2} = 0 \quad \text{in} \quad [-L_1, 0], \\ &- D_1 \frac{\partial c_1}{\partial x} = 0 \qquad \text{at} \quad x = -L_1, \\ &c_1 = C_1 \qquad\qquad \text{at} \quad t = 0, \end{aligned} \tag{2.1}$$

where D_1 is the drug diffusivity in the coating.

Let us now consider the drug dynamics in the wall (second layer). In principle, drug diffusion occurs from the coating towards both the lumen and the adventitia. Therefore an inner double layer system (lumenal side (*lum*)) and an outer double layer system (adventitial side (*adv*)) have to be distinguished. The relative importance of them depends on the penetration depth of the stent, but the adventitial side is generally larger in size and deemed more relevant from a clinical point of view (Fig. 3). Even though the results in the sequel of the paper are mainly referred to it, the following analysis is general and applies to both inner and outer sides.

At adventitial side, being $L_2 \gg L_1$, the concentration c_2 at $x = L_2$ does not change as the time increases and hence it remains equal to its initial value, namely zero. Similarly, in the case of the lumenal side, concentration is nearly zero, because of the extremely high mass transfer coefficient of the blood stream (*washout*). Therefore, in both cases, we end up with an homogeneous boundary condition of the first kind at $x = L_2$ leading to a fraction of drug lost in the tissues adjacent to the adventitia and a fraction dispersed in the lumen.

In general, mass transport in the wall is not governed by diffusion only, but convection is equally important and an advective transport term is added into the model. Thus, we have the following equations:

$$\begin{aligned} &\frac{\partial c_2}{\partial t} + \frac{\partial}{\partial x}\left(\frac{\alpha_2 u_2}{\epsilon_2} c_2 - D_2 \frac{\partial c_2}{\partial x}\right) = 0 \quad \text{in} \quad [0, L_2], \\ &c_2 = 0 \qquad\qquad\qquad\qquad\quad \text{at} \quad x = L_2, \\ &c_2 = 0 \qquad\qquad\qquad\qquad\quad \text{at} \quad t = 0, \end{aligned} \tag{2.2}$$

where D_2 is the drug diffusion coefficient in the wall and ϵ_2 its porosity. The coefficient α_2 is the so-called hindrance coefficient in the x-direction [9]. Finally, $u_2(x,t)$ denotes the volume-averaged filtration velocity of the plasma over a cross section. Such a variable is not known a priori and constitutes a strong coupling term with the fluid-dynamics. In the present case, however, it may simply be estimated as follows.

2.1. Plasma convection

For the unidirectional flow of an isothermal and incompressible fluid in a porous medium the velocity is time independent. The mass conservation gives $u_2(x) = U_2 = const$ in $[0,L_2]$. Assuming the plasma viscosity μ_2 and the wall permeability K_2 as constants, integration of Darcy equation over $[0,L_2]$ gives [14]:

$$U_2 = \frac{\Delta p}{\mu_2 L_2 / K_2} \tag{2.3}$$

In human medium sized arteries, the pressure difference between lumen and adventitia, at normal conditions, does not exceed 100 mmHg and hence the numerator of Eq. (2.3) is less than that. Consequently $U_2 \approx 10^{-6}$ cm/s. By a scaling analysis, the orders of magnitude of the convective and diffusive terms in (2.2) are estimated [10]:

$$\frac{\alpha_2 U_2 c_2}{\epsilon_2} = \mathrm{O}(C_1 U_2), \quad D_2 \frac{\partial c_2}{\partial x} = \mathrm{O}\left(\frac{C_1 D_2}{L_2}\right). \tag{2.4}$$

In the present application D_2/L_2 is one order (resp. three orders) of magnitude larger than U_2 at the adventitial side (resp. lumenal side) and the convective term remains negligible in comparison with the diffusive one. This result is also confirmed by Zunino in Ref. [9], where it is shown that after 6 h up to 76% of heparin is lost into the blood for the case of finite filtration velocity, versus a 72% lost in the case without it.

2.2. Interface conditions

To close the previous system of Eqs. (2.1) and (2.2), the conditions at the interface $x = 0$ (the so-called inner boundary conditions) have to be assigned. One of them is obtained by imposing continuity of the mass flux:

$$D_1 \frac{\partial c_1}{\partial x} = D_2 \frac{\partial c_2}{\partial x} \quad \text{at} \quad x = 0. \tag{2.5}$$

Also, to slow down the drug release rate, a permeable membrane (called *topcoat*) of permeability P (cm/s) is located at the interface ($x = 0$) between the coating and the arterial wall. A continuous mass flux passes through it orthogonally to the coating film with a possible concentration jump. In the present case, the mass transfer through the topcoat can be described using the second Kedem–Katchalsky equation [9,13,15]. Thus, the continuous flux of mass passing across the membrane normally to the coating is expressed by

$$-D_1 \frac{\partial c_1}{\partial x} = P(c_1' - c_2') \quad \text{at} \quad x = 0, \tag{2.6}$$

or, alternatively,

$$-D_2 \frac{\partial c_2}{\partial x} = P(c_1' - c_2') \quad \text{at} \quad x = 0, \tag{2.7}$$

In Eqs. (2.6) and (2.7) the fluid-phase concentration c' is used. This is related to the volume-averaged concentration c through the formula $c' = \dfrac{c}{k\epsilon}$, where k is the partition coefficient [3,9]. As one of the last three equations is redundant, we can choose any two of them, for example Eqs. (2.5) and (2.7).

Note that, when $P \to \infty$, Eqs. (2.6) and (2.7) reduce to $c_1' = c_2'$. This equality contrasts with what occurs at the interface of two-layer heat conduction problems where the temperatures across the interface are always equal, if the two bodies are in perfect thermal contact. In mass diffusion, instead, because the media are porous and drug is partly dissolved in the fluid and partly bound with the polymeric matrix in solid phase, only the fluid-phase concentration enters to the flux dynamics.

2.3. Dimensionless form

Let us define the following nondimensional variables and constants:

$$\bar{x}=\frac{x}{L_2},\quad \bar{t}=\frac{D_2}{L_2^2}t,\quad \bar{c}_1=\frac{c_1}{C_1},\quad \bar{c}_2=\frac{c_2}{C_1},$$
$$\gamma=\frac{D_1}{D_2},\quad L=\frac{L_1}{L_2},\quad \phi=\frac{PL_2}{D_2k_2\epsilon_2},\quad \sigma=\frac{k_1\epsilon_1}{k_2\epsilon_2}. \tag{2.8}$$

By setting

$$\bar{x}\to x,\quad \bar{t}\to t,\quad \bar{c}_1\to c_1,\quad \bar{c}_2\to c_2, \tag{2.9}$$

and neglecting the convective term in Eq. (2.2), the two differential problems (2.1) and (2.2) with B.C.'s (2.5) and (2.7) may be rewritten in a dimensionless form as

$$\begin{aligned}
&\frac{\partial c_1}{\partial t}-\gamma\frac{\partial^2 c_1}{\partial x^2}=0 \quad \text{in} \quad [-L,0],\\
&\frac{\partial c_1}{\partial x}=0 \qquad\qquad \text{at} \quad x=-L,\\
&\gamma\frac{\partial c_1}{\partial x}=\frac{\partial c_2}{\partial x} \qquad \text{at } x=0,\\
&c_1=1 \qquad\qquad \text{at} \quad t=0,
\end{aligned} \tag{2.10}$$

$$\begin{aligned}
&\frac{\partial c_2}{\partial t}-\frac{\partial^2 c_2}{\partial x^2}=0 \qquad \text{in} \quad [0,1],\\
&-\frac{\partial c_2}{\partial x}=\phi\left(\frac{c_1}{\sigma}-c_2\right) \qquad \text{at} \quad x=0,\\
&c_2=0 \qquad\qquad \text{at} \quad x=1,\\
&c_2=0 \qquad\qquad \text{at} \quad t=0.
\end{aligned} \tag{2.11}$$

Note that if a linear mass consumption term (due to a drug binding and chemical effects) is present in the wall layer, the (2.10) and (2.11) can be written in the same form through an appropriate transformation.

The IBVP problem (2.10) and (2.11) is analogous to the problem of transient heat conduction between two-slab shaped regions of different thermal properties, when a temperature jump is initially present, with the only exception of the inner boundary condition in Eqs. (2.11), as has already been stated previously. For this reason, the analytical solution procedure developed in [12] for the transient heat conduction in a one-dimensional composite slab will be adapted to our problem in the next sections.

3. Solution of the governing equations

In general, the solution of a linear boundary value problem can be given in a short- and in a long-time form (see [16, chapter 5]). The former arises from the application of Laplace transform and the long-time form is based on the method of separation of variables. They are two mathematically equivalent expressions of the unique solution, which are complementary in terms of computational efficiency. The short-time form requires only a few terms for small values of the time and the long-time expression needs only a few terms for large values of the dimensionless time [16]. Being the Laplace transform method applicable only to solve problems of composite media of semi-infinite thickness, the solution to the (2.10) and (2.11) cannot be of the short-time form. Hence it will be obtained by separation of variables

$$c_i(x,t)=X_i(x)G_i(t),\quad i=1,2. \tag{3.1}$$

Eqs. (2.10) and (2.11) yield the ODE's

$$\frac{1}{\gamma}\frac{G_1'}{G_1}=-\lambda_1^2,\quad \frac{G_2'}{G_2}=-\lambda_2^2 \tag{3.2}$$

having as solution

$$G_1(t)=\mathrm{e}^{-\gamma\lambda_1^2 t},\quad G_2(t)=\mathrm{e}^{-\lambda_2^2 t}, \tag{3.3}$$

and the Sturm–Liouville eigenvalue system:

$$X_1''=-\lambda_1^2X_1 \quad \text{in} \quad [-L,0], \tag{3.4}$$
$$X_1'=0 \qquad \text{at} \quad x=-L, \tag{3.5}$$
$$\gamma X_1'=X_2' \qquad \text{at} \quad x=0, \tag{3.6}$$

$$X_2''=-\lambda_2^2X_2 \qquad \text{in} \quad [0,1], \tag{3.7}$$
$$X_2=0 \qquad \text{at} \quad x=1, \tag{3.8}$$
$$-X_2'+\phi X_2=\frac{\phi}{\sigma}X_1 \quad \text{at} \quad x=0, \tag{3.9}$$

obtained by setting $G_1=G_2$ [17], that implies

$$\lambda_1=\frac{1}{\sqrt{\gamma}}\lambda_2. \tag{3.10}$$

The general solution of the ordinary differential Eqs. (3.4) and (3.7) is

$$\begin{aligned}
X_1(x)&=a_1\cos(\lambda_1 x)+b_1\sin(\lambda_1 x),\\
X_2(x)&=a_2\cos(\lambda_2 x)+b_2\sin(\lambda_2 x),
\end{aligned} \tag{3.11}$$

where the eigenvalues λ_i and the unknown coefficients a_i and b_i may be computed by imposing the outer and inner boundary conditions as follows. From Eqs. (3.5) and (3.8), we have

$$a_1\sin(\lambda_1 L)+b_1\cos(\lambda_1 L)=0, \tag{3.12}$$
$$a_2\cos(\lambda_2)+b_2\sin(\lambda_2)=0. \tag{3.13}$$

From the interface conditions (3.6) and (3.9), it follows:

$$\gamma b_1\lambda_1=b_2\lambda_2, \tag{3.14}$$
$$-b_2\lambda_2+\phi a_2=\frac{\phi}{\sigma}a_1. \tag{3.15}$$

Eqs. (3.12)–(3.15) form a system of four homogeneous linear algebraic equations in the four unknowns a_1, b_1, a_2 and b_2. To get a solution different from the *trivial* one $(0,0,0,0)$, it is needed that the determinant of the coefficient matrix associated with the above system be equal to zero, that is:

$$\varphi(\lambda_2)=\sigma\sqrt{\gamma}(\lambda_2+\phi\tan\lambda_2)\tan\left(\frac{L}{\sqrt{\gamma}}\lambda_2\right)-\phi=0. \tag{3.16}$$

If the above transcendental equation (eigencondition) in λ_2 is satisfied, the coefficients may be taken as

$$a_1 = -\sigma\left(\tan\lambda_2 + \frac{\lambda_2}{\phi}\right)b_2, \tag{3.17}$$

$$b_1 = \frac{1}{\sqrt{\gamma}}b_2, \tag{3.18}$$

$$a_2 = -(\tan\lambda_2)b_2, \tag{3.19}$$

where the multiplicative constant b_2 will be determined through the initial condition (see below). Let us note that φ depends on the four parameters σ, ϕ, L, γ, it is an odd function and its roots (eigenvalues) are infinite, real and distinct (see Appendix A.3). We also remark that φ has an infinite number of singularity points, say

$$\mu_j = \pi\left(\frac{1}{2}+j\right), \quad \nu_j = \frac{\pi\sqrt{\gamma}}{L}\left(\frac{1}{2}+j\right), \qquad j = 0,1,2,\ldots \tag{3.20}$$

Differently than in heat transfer models [18] – due to the present interface condition (3.9) – the function φ is not monotone and the property that each root is located exactly between any two adjacent asymptotes is not satisfied. In correspondence of each eigenvalue λ_{2m} ($m = 1,2,\ldots$) solution of Eq. (3.16), an associated λ_{1m} is found (see Eqs. (3.10)). Subsequently, the constants a_{1m}, b_{1m} and a_{2m} are obtained from (3.17), (3.18) and (3.19) respectively, and thus the corresponding eigenfunctions X_{1m} and X_{2m} defined in Eqs. (3.11) may be written as

$$\begin{aligned} X_{1m} &= b_{2m}\widetilde{X}_{1m} \\ &= b_{2m}\left[-\sigma\left(\tan(\lambda_{2m}) + \frac{\lambda_{2m}}{\phi}\right)\cos(\lambda_{1m}x) + \frac{1}{\sqrt{\gamma}}\sin(\lambda_{1m}x)\right], \end{aligned} \tag{3.21}$$

$$\begin{aligned} X_{2m} &= b_{2m}\widetilde{X}_{2m} \\ &= b_{2m}[-\tan(\lambda_{2m})\cos(\lambda_{2m}x) + \sin(\lambda_{2m}x)]. \end{aligned} \tag{3.22}$$

Furthermore, the corresponding time-variable functions G_{1m} and G_{2m} defined by Eqs. (3.3) are computed, using (3.10), as

$$G_{1m} = G_{2m} = \mathrm{e}^{-\lambda_{2m}^2 t}. \tag{3.23}$$

Finally, the complete solution of the problem is given by a linear superposition of the fundamental solutions (3.21) and (3.22) in the form

$$\begin{aligned} c_1(x,t) &= \sum_{m=1}^{\infty} A_m \widetilde{X}_{1m}(x)\mathrm{e}^{-\lambda_{2m}^2 t}, \\ c_2(x,t) &= \sum_{m=1}^{\infty} A_m \widetilde{X}_{2m}(x)\mathrm{e}^{-\lambda_{2m}^2 t}, \end{aligned} \tag{3.24}$$

with $A_m := b_{2m}$.

3.1. Application of the initial condition

By evaluating c_1 in (3.24) at $t = 0$ and multiplying it by $\widetilde{X}_{1n}$, after integration we get

$$\int_{-L}^{0} \sum A_m \widetilde{X}_{1m}\widetilde{X}_{1n}\,\mathrm{d}x = \int_{-L}^{0} \widetilde{X}_{1n}\,\mathrm{d}x, \quad n = 1,2,\ldots \tag{3.25}$$

Similarly in the interval [0,1], we have

$$\int_{0}^{1} \sum A_m \widetilde{X}_{2m}\widetilde{X}_{2n}\,\mathrm{d}x = 0, \quad n = 1,2,\ldots \tag{3.26}$$

By combining Eqs. (3.25) and (3.26) and by using the orthogonality property (A.1) we have

$$A_m\left(\int_{-L}^{0} \widetilde{X}_{1m}^2\,\mathrm{d}x + \sigma\int_{0}^{1} \widetilde{X}_{2m}^2\,\mathrm{d}x\right) = \int_{-L}^{0} \widetilde{X}_{1m}\,\mathrm{d}x, \tag{3.27}$$

where the term in brackets on the l.h.s. is the norm $\widetilde{N}_m = \dfrac{N_m}{b_{2m}^2}$ with N_m given in Eq. (A.2). Bearing in mind Eq. (3.21) and integrating from $-L$ to 0, we have

$$A_m = \frac{-\sigma\left(\tan\lambda_{2m} + \dfrac{\lambda_{2m}}{\phi}\right)\sin(\lambda_{1m}L) + \dfrac{1}{\sqrt{\gamma}}(\cos(\lambda_{1m}L) - 1)}{\widetilde{N}_m\lambda_{1m}}, \quad m = 1,2,\ldots \tag{3.28}$$

3.2. Physical quantities and operational conditions

From Eq. (3.24) it is possible to compute the dimensionless drug mass (per unit of area) in both coating and wall layers as function of time as

$$M_1(t) = \int_{-L}^{0} c_1(x,t)\,\mathrm{d}x, \quad M_2(t) = \int_{0}^{1} c_2(x,t)\,\mathrm{d}x, \tag{3.29}$$

obtaining

$$M_1(t) = \sum_{m=1}^{\infty} A_m^2 \widetilde{N}_m \mathrm{e}^{-\lambda_{2m}^2 t}, \tag{3.30}$$

$$M_2(t) = \sum_{m=1}^{\infty} A_m\left(\frac{-\tan(\lambda_{2m})\sin(\lambda_{2m}) - \cos(\lambda_{2m}) + 1}{\lambda_{2m}}\right)\mathrm{e}^{-\lambda_{2m}^2 t}. \tag{3.31}$$

In particular $M_1(0) = L$ and $M_2(0) = 0$.

Similarly, the dimensionless mass flux and jump of concentration at interface are respectively

$$J(t) = -\gamma\frac{\partial c_1}{\partial x}(0,t) = -\frac{\partial c_2}{\partial x}(0,t) = -\sum_{m=1}^{\infty} A_m\lambda_{2m}\mathrm{e}^{-\lambda_{2m}^2 t} \tag{3.32}$$

$$S(t) = (c_1 - c_2)(0,t) = \sum_{m=1}^{\infty} A_m\left[(1-\sigma)\tan(\lambda_{2m}) - \sigma\frac{\lambda_{2m}}{\phi}\right]\mathrm{e}^{-\lambda_{2m}^2 t}. \tag{3.33}$$

In particular $J(0) \to \infty$ and $S(0) = 1$.

All the previous variables characterize the *performance* of the drug elution process and can be used for its optimization.

4. Computational results

The following physical parameters are considered for computational experiments:

$L_1 = 5 \times 10^{-4}$ cm, $L_2 = 10^{-2}$ cm,
$P = 10^{-6}$ cm/s, $D_1 = 10^{-10}$ cm^2/s, $D_2 = 7 \times 10^{-8}$ cm^2/s
$k_1 = 1$, $k_2 = 1$, $\epsilon_1 = 0.1$, $\epsilon_2 = 0.61$.

These parameters have been chosen according to a physical basis and in agreement with the typical scales in DES and data in literature for the arterial wall and heparin drug in the coating layer [2,3,19].

The physical problem apparently depends on a large number of parameters, each of them may vary in a finite range, and there is a variety of different limiting cases. As a matter of fact, they cannot be chosen independently from each other, but they are related by some compatibility condition to give rise a well-posed model. However the problem depends only on the four nondimensional operational parameters defined by Eq. (2.8). In the present case, their values are

$$\phi = 0.234, \quad \sigma = 0.164, \quad L = 0.05, \quad \gamma = 0.0014. \tag{4.1}$$

The four ratios ϕ, σ, L, γ are the only intrinsic parameters of the problem and they are used as mean values for a set of numerical simulations.

First of all, Eq. (3.16) is solved numerically with a bisection-like method by using intervals limited by the points μ_j and ν_j, $j = 0, 1, 2, \ldots$ (see Eq. (3.20)) and midpoints between them, as starting guess (routine *fzero* of MATLAB,with accuracy of 10^{-8}). In particular, the first roots of Eq. (3.16) are given in Table 1. The damping factor, defined as $\delta_m(t) = \exp(-\gamma\lambda_{1m}^2 t)$, measures the attenuation of the various terms in summations (3.24) and is listed in the same table. Its values indicate a fast (exponential) convergence of the solu-

Table 1
First eigenvalues λ_{2m} of Eq. (3.16), and corresponding damping factors $\delta(t)$ at three different times

m	λ_{2m}	$\delta_m(0.01)$	$\delta_m(0.1)$	$\delta_m(1)$	$\max_x\lvert A_m\widetilde{X}_{1m}\rvert$	$\max_x\lvert A_m\widetilde{X}_{2m}\rvert$
1	1.153	0.986	0.875	0.264	1.2485	0.1064
2	1.580	0.975	0.778	0.082	0.0232	0.0755
3	3.490	0.885	0.295	5.098×10^{-6}	0.4206	0.0168
4	4.712	0.800	0.108	2.262×10^{-10}	0.0001	0.0007
5	5.823	0.712	0.033	1.864×10^{-15}	0.2503	0.0104
6	7.841	0.540	2.134×10^{-3}	$<10^{-20}$	0.0071	0.0180
7	8.164	0.513	1.272×10^{-3}	$<10^{-20}$	0.1702	0.0206
8	10.474	0.333	1.717×10^{-5}	$<10^{-20}$	0.1338	0.0097
9	11.003	0.297	5.511×10^{-6}	$<10^{-20}$	0.0022	0.0091
10	12.813	0.193	7.406×10^{-8}	$<10^{-20}$	0.1092	0.0040
20	26.687	8.071×10^{-4}	$<10^{-20}$	$<10^{-20}$	0.0042	0.0066
40	52.717	8.518×10^{-13}	$<10^{-20}$	$<10^{-20}$	0.0165	0.0004

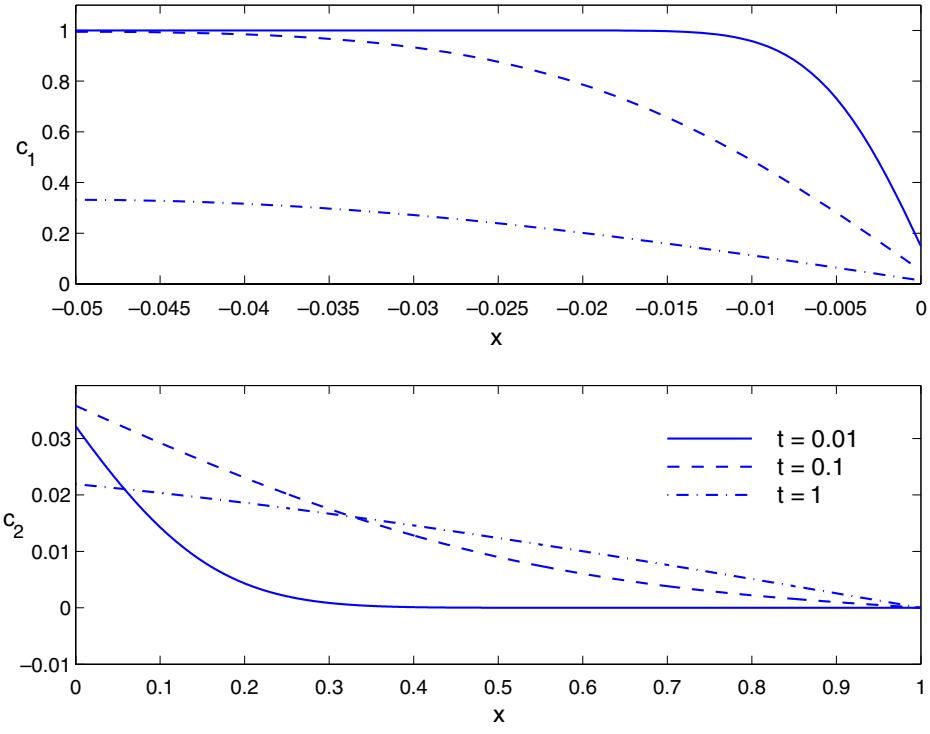

Fig. 4. Drug concentration profiles in the coating (above) and in the wall (below) for three times (note the different space scales).

tion. Because of that, the series (3.24) will be truncated at a finite number of terms. Such a number can be found in accordance with the accuracy desired at the time of interest. Being $\max_x|A_m\widetilde{X}_{im}| < 1$ for any $i = 1,2$, $m > 1$ (see Table 1), to reach an accuracy of 10^{-r}, it is sufficient to consider a finite series summation up to the index $M_t > 1$ such that

$$\lambda_{2Mt} > \sqrt{\frac{r\ln 10}{t}},$$

and the series is truncated at the first M_t terms. M_t is adaptively changed during computations: its values drop from $M_t = 40$ at the shorter times, down to $M_t = 5$ at higher times.

The concentration profiles for three values of time are displayed in Fig. 4: drug is eluting from coating to the wall, with concentration decaying in time. Because of the different material properties of the substrates, at first instants c_1 and c_2 exhibit a steep boundary layer near $x = 0$, which disappears at later times.

Fig. 5 shows that drug mass in the coating layer M_1 is monotonically decreasing, while mass in the wall M_2, first increasing to a maximum M_2^* at time t^*, decreases to zero with the same rate of M_1. Since drug is absorbed at $x = 1$, the total mass is not preserved and tends to zero at time large enough.

The mass flux $J(t)$ and the concentration jump $S(t)$ at the interface are depicted in Fig. 6. Both quantities evidence a sudden change at first instants and then an asymptotic vanishing. There is a finite instant where S reaches a minimum, namely the same time where M_2 reaches its maximum M_2^*.

4.1. Validation of the results

Comparison with numerical results of other models in 3D complex geometries has shown a good agreement. In particular, a certain discrepancy in the values of concentrations occurs at small times ($t \leqslant 0.05$), since the boundary layer at the interface is not sufficiently resolved. For example, at $x = 0$ and $t = 0.01$ the maximum absolute error is 0.06 for c_1 and 0.0018 for c_2 [5].

We also compare the fraction of drug mass lost partly at the lumen (θ_{lum}) and partly external to the adventitia (θ_{adv}) [9]. They are defined respectively as:

$$\theta_{\text{lum}}(t) = \frac{[M_1(0) - (M_1(t) + M_2(t))]_{\text{lum}}}{M_{\text{tot}}(0)},$$

$$\theta_{\text{adv}}(t) = \frac{[M_1(0) - [(M_1(t) + M_2(t))]_{\text{adv}}}{M_{\text{tot}}(0)},$$

where $M_{\text{tot}}(0)$ is the total (lumenal + adventitial side) initial mass. It is shown how the mass lost in the lumen is strongly influenced by the penetration depth (L_2^{lum}) of the stent, when all the other parameters are kept constant (Table 2). Note that θ_{adv} is absent in model [9], since a zero mass flux is imposed as external boundary condition.

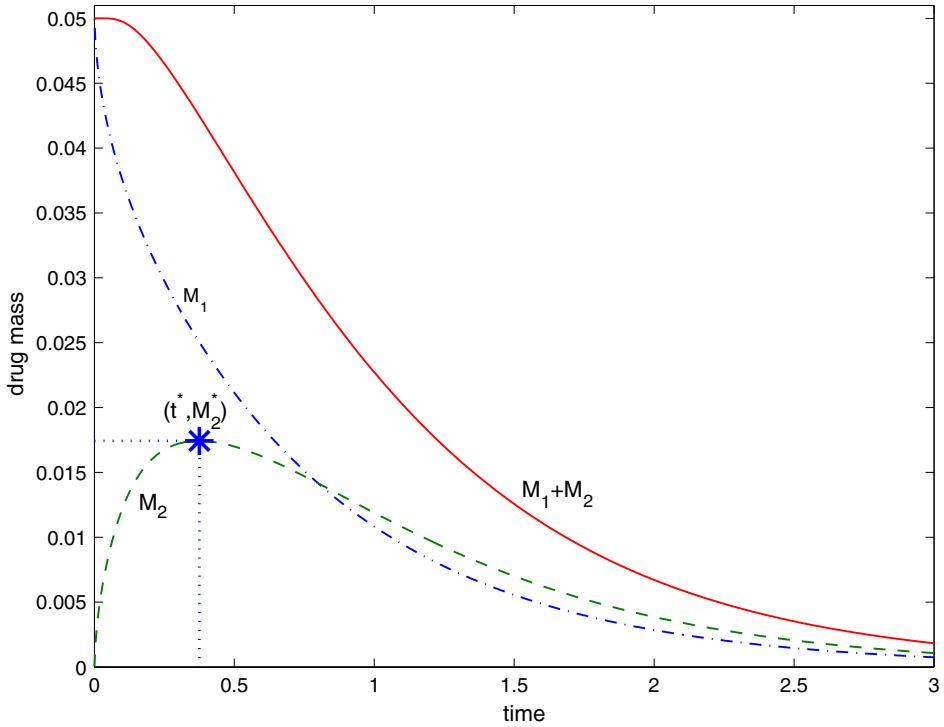

Fig. 5. Dimensionless drug mass in the coating (···), in the wall (---), and total mass (—) as function of time. In the coating, drug mass M_1 is monotonically decreasing, while in the wall there is a characteristic time t^* at which the drug reaches a maximum peak M_2^*. Due to the absorption at the wall, drug is not preserved and vanishes at a time large enough.

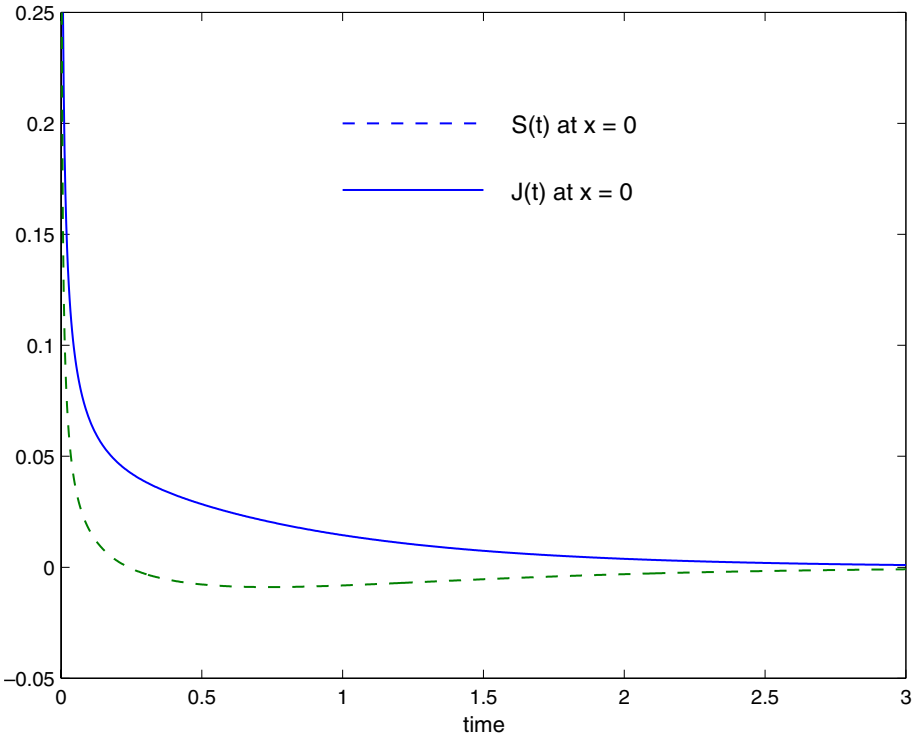

Fig. 6. Mass flux (continuous line) and concentration jump (dashed line) at the interface $x = 0$ as function of time.

Table 2
Percentage of drug mass lost at lumenal (θ_{lum}) and advential (θ_{adv}) sides at nominal ($L_2^{lum} = 10$ μm) and at two off-nominal configurations. Mass are computed in dimensional form and compared with those in the model of Zunino [9], showing a strong influence of the penetration depth (L_2^{lum}) on the drug elution and dispersion

Time	Present work			Ref. [9]	
	L_2^{lum} (μm)	θ_{lum} (%)	θ_{adv} (%)	θ_{lum} (%)	θ_{adv} (%)
3000 s (50 min)	10	34.9	8.3	53	0
	5	91.7	4.3		
	2.5	94	2.2		
10,000 s (≈2 h 45 min)	10	64	9.1	66	0
	5	95.2	4.7		
	2.5	97.5	2.4		
20,000 s (≈5 h 30 min)	10	81.5	9.1	72	0
	5	95.2	4.8		
	2.5	97.6	2.4		

4.2. Sensitivity analysis

Design parameters governing the drug release can be screened by analyzing the solution dependence and the sensitivity on the groups L, γ, ϕ and σ when they are varied in a limited realistic range one at a time around the mean values in Eq. (4.1), with the others fixed. Results from numerical simulations are shortly reported below.

- *Dependence on* L: Increasing L, higher values for the concentrations c_1 and c_2 at the interface are obtained at larger times. A slower drug release is exhibited in both layers at larger L. The solution is shown very sensitive to L.
- *Dependence on* γ: The drug is released faster with γ in both layers. The mass M_1 is decaying with γ, while M_2 shows an increased value of the peak, followed by a faster decay. The solution is quite sensitive to γ.
- *Dependence on* σ: Increasing σ we have a raising of c_1 and a reduction of c_2 at the interface for initial times. The mass M_1 is slightly increased at larger times, while the peak for M_2 is reduced and occurs at later instants.
- *Dependence on* ϕ: Associated with a high ϕ, a reduction of c_1 and an increase of c_2 at the interface are reported only at first times. When ϕ is decreased, the peak of M_2 lowers and is attained at a larger time. Consequently, the drug release is slower at lower ϕ. For values of $\phi > 1$ the solution does not change significantly.

4.3. Drug-delivery indicators

For novel coating design and comparative purposes, it is desirable to search for simple quantitative *indicators* of the drug dynamics. Several scalar indexes can be defined, for example:

1. Emptying time t_E, namely the time at which the drug mass drops below a given amount in the coating layer (1) with respect to the initial mass (in the simulations $M_1(t_E) = 0.001 M_1(0) = 0.001 L$, where the expression for $M_1(t)$ is given by Eq. (3.30)).
2. Mass M_2 at a given time.

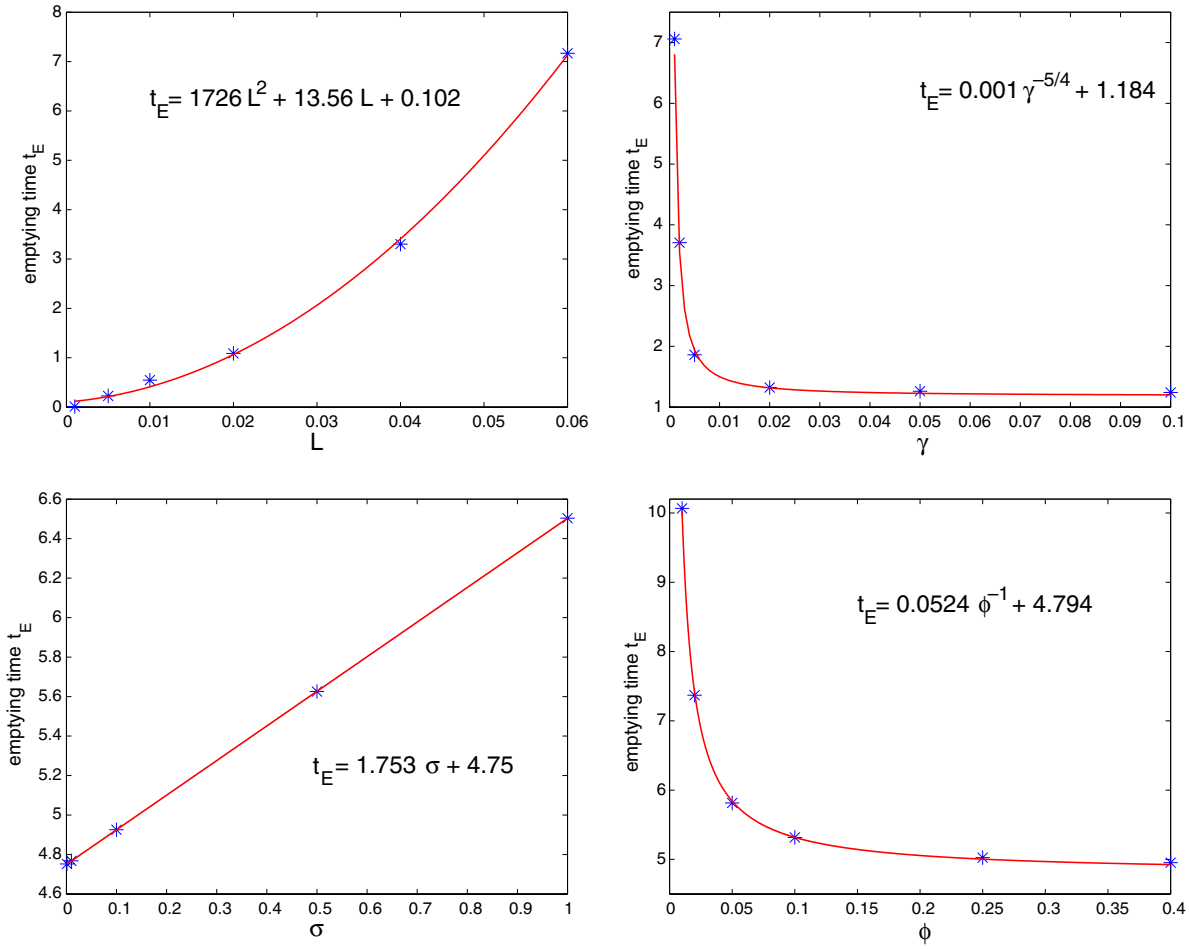

Fig. 7. Variation of the indicator (1) (emptying time in coating) with γ, L, σ and ϕ in a typical range. In each plot, only one parameter is changed, and the other three hold as in Eq. (4.1). Starred points are results from simulation, continuous lines are fitting curves.

3. Magnitude (m_2) and uniformity (s_2) of the wall concentration c_2.
4. Location and value of the peak in the wall layer (2). Time t^* and maximum value M_2^* are possible pointers of drug release kinetics.

Depending on the specific optimizing purposes and technological limitations, one or a combination of some of them may provide significant and useful hints.

The indicators (3) are computed by first averaging c_2 (and its derivative) over the wall length and then considering their maximum values in time. The variation of both indexes with each of the four parameters is monotone, and has the same trend. In particular, a reduction of one order of magnitude on ϕ (resp. γ) implies a reduction of 25% (resp. 55%) on s_2 and of 23% (resp. 67%) on m_2.

The indicator (1) seems to be more promising and its sensitivity is fully investigated. The dependence of the emptying time on γ, L, ϕ and σ is shown in Fig. 7 with one parameter varied in a convenient interval and the other three fixed as in Eq. (4.1): in all cases the variation is monotone and the maximum value is reached at one end of the interval. The computed data are fitted with appropriate functions. In particular, t_E shows a linear rising with σ and a quadratic behaviour with L. On the other hand, t_E decreases as ϕ^{-1} and as $\gamma^{-\frac{5}{4}}$. As a consequence, large values of L and σ and small values of γ and ϕ, compatible with technological requirements and implantation limits, guarantee the best drug release performance.

5. Conclusions

The release of a substance in a living tissue for therapeutic purposes is becoming quite common in medicine nowadays, through drug delivery devices. Drug-eluting stents are revealed a promising technique for healing the vascular wall and for the treatment of atherosclerosis and restenosis. However, the mechanism of release is quite complex and depends on many concurrent biochemical, physical and individual factors. The model presented here, although some simplifying assumptions, is able to simulate and predict the dynamics of a drug through a two-layered medium and to estimate the dose absorption rate and is solved in a closed form. An advantage of the methodology is that the procedure is analytical and the only computational cost consists in searching the roots of the eigenvalue equation. The model can be easily extended to a multi-layered structure, including both a more realistic wall configuration and

a novel design for multi-coating DES. In addition, the mathematical formulation is able to incorporate the drug consumption effect due to the tissue cell binding. The application of the dimensional analysis to the governing equations has indicated that the dynamics of a drug through an eluting stent is fully controlled by only four dimensionless operational parameters. Numerical experiments have been extensively carried out over several typical configurations. Results have shown the influence of the solution on each single parameter, in particular the ratios between thickness and drug diffusivities of the two layers. Also, some biomechanical indicators, such as the emptying time of the coating, are suggested to obtain an optimal drug-elution and a desired tissue concentration.

Acknowledgements

The authors wish to thank Dr. M. Prosi and Dr. P. Zunino for their valuable suggestion and criticism in the development of this work.

Appendix A

A.1. Orthogonality

We shall prove that the eigenfunction system (X_1, X_2) satisfies the following orthogonality property:

$$\int_{-L}^{0} X_{1n}X_{1m}\,\mathrm{d}x + \sigma\int_{0}^{1} X_{2n}X_{2m}\,\mathrm{d}x = \begin{cases} 0 & \text{for} \quad m \neq n, \\ N_m & \text{for} \quad m = n, \end{cases} \tag{A.1}$$

with the expression for the norm N_m given by

$$N_m = b_{2m}^2\left\{\frac{1}{2}\left[\left(\left(\frac{a_{1m}}{b_{2m}}\right)^2 + \left(\frac{b_{1m}}{b_{2m}}\right)^2\right)L - \frac{a_{1m}b_{1m}}{b_{2m}^2\lambda_{1m}}\right] + \frac{\sigma}{2}\left[\left(\left(\frac{a_{2m}}{b_{2m}}\right)^2 + 1\right) + \frac{a_{2m}}{b_{2m}\lambda_{2m}}\right]\right\} \tag{A.2}$$

(see subsection A.2 for the proof). Note that the all ratios in the square brackets are expressible in terms of eigenvalues through Eqs. (3.17), (3.18) and (3.19).

Let us consider two different eigenvalues λ_{1m} and λ_{1n} and the corresponding eigenfunctions X_{1m}, X_{1n}. Multiplying Eq. (3.4) by X_{1n} and integrating:

$$\lambda_{1m}^2\int_{-L}^{0} X_{1m}X_{1n}\,\mathrm{d}x = -\int_{-L}^{0} X''_{1m}X_{1n}\,\mathrm{d}x = -[X'_{1m}X_{1n}]_{-L}^{0} + \int_{-L}^{0} X'_{1m}X'_{1n}\,\mathrm{d}x. \tag{A.3}$$

Similarly, for the eigenvalue λ_{1n}

$$\lambda_{1n}^2\int_{-L}^{0} X_{1n}X_{1m}\,\mathrm{d}x = -\int_{-L}^{0} X''_{1n}X_{1m}\,\mathrm{d}x = -[X'_{1n}X_{1m}]_{-L}^{0} + \int_{-L}^{0} X'_{1n}X'_{1m}\,\mathrm{d}x. \tag{A.4}$$

Subtracting Eq. (A.4) from Eq. (A.3) we have

$$(\lambda_{1m}^2 - \lambda_{1n}^2)\int_{-L}^{0} X_{1n}X_{1m}\,\mathrm{d}x = -[X'_{1m}X_{1n}]_{-L}^{0} + [X'_{1n}X_{1m}]_{-L}^{0}. \tag{A.5}$$

By replacing the expression of the first of Eqs. (3.11) of the eigenfunctions and by using Eq. (3.12) we obtain

$$(\lambda_{1m}^2 - \lambda_{1n}^2)\int_{-L}^{0} X_{1n}X_{1m}\,\mathrm{d}x = a_{1m}b_{1n}\lambda_{1n} - a_{1n}b_{1m}\lambda_{1m}. \tag{A.6}$$

Repeating a similar procedure for the eigenvalues λ_{2m}, λ_{2n} and for the eigenfunctions X_{2m}, X_{2n}, we get

$$(\lambda_{2m}^2 - \lambda_{2n}^2)\int_{0}^{1} X_{2n}X_{2m}\,\mathrm{d}x = -[X'_{2m}X_{2n}]_{0}^{1} + [X'_{2n}X_{2m}]_{0}^{1} \tag{A.7}$$

and by using the second of Eqs. (3.11) and Eq. (3.13) we have

$$(\lambda_{2m}^2 - \lambda_{2n}^2)\int_{0}^{1} X_{2n}X_{2m}\,\mathrm{d}x = a_{2n}b_{2m}\lambda_{2m} - a_{2m}b_{2n}\lambda_{2n}. \tag{A.8}$$

By summing up Eq. (A.6) multiplied by γ and Eq. (A.8) multiplied by σ, and by using Eqs. (3.10), (3.18) and (3.15) we have

$$(\lambda_{2m}^2 - \lambda_{2n}^2)\left(\int_{-L}^{0} X_{1n}X_{1m}\,\mathrm{d}x + \sigma\int_{0}^{1} X_{2n}X_{2m}\,\mathrm{d}x\right) = 0, \tag{A.9}$$

which immediately proves Eq. (A.1).

A.2. Normalization integral

We shall now prove that the norm N_m has the expression given by Eq. (A.2).

Multiplying Eq. (3.4) by X_{1m} and integrating we have

$$\lambda_{1m}^2\int_{-L}^{0} X_{1m}^2\,\mathrm{d}x = -\int_{-L}^{0} X''_{1m}X_{1m}\,\mathrm{d}x = -[X'_{1m}X_{1m}]_{-L}^{0} + \int_{-L}^{0}(X'_{1m})^2\,\mathrm{d}x. \tag{A.10}$$

Multiplying the first of Eqs. (3.11) by λ_{1m} and summing its square with the square of

$$X'_{1m} = -a_{1m}\lambda_{1m}\sin(\lambda_{1m}x) + b_{1m}\lambda_{1m}\cos(\lambda_{1m}x),$$

we get

$$(\lambda_{1m}X_{1m})^2 + (X'_{1m})^2 = \lambda_{1m}^2(a_{1m}^2 + b_{1m}^2). \tag{A.11}$$

Integration of both side of the above equation leads to

$$\lambda_{1m}^2\int_{-L}^{0} X_{1m}^2\,\mathrm{d}x + \int_{-L}^{0}(X'_{1m})^2\,\mathrm{d}x = \lambda_{1m}^2(a_{1m}^2 + b_{1m}^2)L. \tag{A.12}$$

Summation of Eqs. (A.10) and (A.12) gives

$$2\lambda_{1m}^2\int_{-L}^{0} X_{1m}^2\,\mathrm{d}x = \lambda_{1m}^2(a_{1m}^2 + b_{1m}^2)L - [X'_{1m}X_{1m}]_{-L}^{0}. \tag{A.13}$$

By using the first of Eqs. (3.11) and Eq. (3.12), the r.h.s can be easily manipulated to get

$$\int_{-L}^{0} X_{1m}^2\,\mathrm{d}x = \frac{L}{2}(a_{1m}^2 + b_{1m}^2) - \frac{a_{1m}b_{1m}}{2\lambda_{1m}}. \tag{A.14}$$

Repeating the same procedure for an eigenfunction X_{2m}

$$\int_0^1 X_{2m}^2\,\mathrm{d}x = \frac{1}{2}(a_{2m}^2 + b_{2m}^2) + \frac{a_{2m}b_{2m}}{2\lambda_{2m}}. \tag{A.15}$$

Substitution of Eqs. (A.14) and (A.15) into Eq. (A.1) for $m = n$ gives the result.

A.3. Reality of the eigenvalues

We first prove that the Eq. (3.16) cannot have a complex root of the form $\lambda_2 = p \pm jq$, where p and q are positive real numbers, and j is the imaginary unit. In fact, if this were possible, we would have two conjugate roots $\lambda_{2m} = p + jq$ and $\lambda_{2n} = p - jq$. Substituting these two complex roots in Eq. (3.11), after some algebraic manipulations, the eigenfunctions may be separated into their real and imaginary parts and rewritten as

$$X_{1r}(x) = R_1(x) \pm jS_1(x), \quad X_{2r}(x) = R_2(x) \pm jS_2(x),$$
$$r = m, n$$

Applying the orthogonality property (A.1) with $m \neq n$, we would have

$$\int_{-L}^0 (R_1^2 + S_1^2)\,\mathrm{d}x + \sigma \int_0^1 (R_2^2 + S_2^2)\,\mathrm{d}x = 0, \tag{A.16}$$

which is impossible as both terms on the l.h.s. of Eq. (A.16) are positive. With a similar argument, we demonstrate that Eq. (3.16) cannot admit purely imaginary roots of the form $\lambda_2 = \pm jq$. In such a case Eq. (A.16) would hold with $R_1 = R_2 = 0$.

References

[1] P.A. Netti, F. Travascio, R.K. Jain, Coupled macromolecular transport and gel mechanics: poroviscoelastic approach, AiChE J. 49 (6) (2003) 1580–1596.

[2] D.V. Sakharov, L.V. Kalachev, D.C. Rijken, Numerical simulation of local pharmacokinetics of a drug after intravascular delivery with an eluting stent, J Drug Target 10 (6) (2002) 507–513.

[3] C. Creel, M. Lovich, E. Edelman, Arterial paclitaxel distribution and deposition, Circ. Res. 86 (8) (2000) 879–884.

[4] C.D.K. Rogers, Drug-eluting stents: role of stent design delivery vehicle and drug selection, Rev. Cardiov. Med. 3 (supp. 5) (2002) S10–S15.

[5] M. Prosi, F. Gervaso, P. Zunino, S. Minisini, L. Formaggia, Numerical simulations of drug release from stents, in: Proc. 7th Int. Symp. on Comp. Meth. in Biomech. and Biomed. Eng., Antibes (FR), 22–25 March, 2006.

[6] N. Yang, K. Vafai, Modelling of low-density lipoprotein (LDL) transport in the artery – effect of hypertension, Int. J. Heat Mass Transf. (2006) 850–867.

[7] L. Ai, K. Vafai, A coupling model for macromolecules transport in a stenosed arterial wall, Int. J. Heat Mass Transf. (2006) 1568–1591.

[8] M.C. Delfour, A. Garon, V. Longo, Modeling and design of coated stents to optimize the effect of the dose, SIAM J. App. Math. 65 (3) (2005) 858–881.

[9] P. Zunino, Multidimensional pharmacokinetic models applied to the design of drug-eluting stents, Cardiov. Eng.: Int. J. 4 (2) (2004).

[10] H.D. Baehr, K. Stephan, Heat Mass Transf., Springer Verlag, Berlin, 1998.

[11] S.R. deGroot, P. Mazur, Non-Equilibrium Thermodynamics, Dover Pub, New York, 1984.

[12] F. de Monte, Transient heat conduction in one-dimensional composite slab. A natural analytical approach, Int. J. Heat Mass Transf. 43 (2000) 3607–3619.

[13] M. Prosi, P. Zunino, K. Perktold, A. Quarteroni, Mathematical and numerical models for transfer of low-density lipoproteins through the arterial walls: a new methodology for the model set up with applications o the study of disturbed lumenal flow, J. Biomech. 38 (2005) 903–917.

[14] A.-R.A. Khaled, K. Vafai, The role of porous media in modeling flow and heat transfer in biological tissues, Int. J. Heat Mass Transf. 46 (2003) 4989–5003.

[15] A. Kargol, M. Kargol, S. Przestalski, The Kedem–Katchalsky equations as applied for describing substance transport across biological membranes, Cell. Mol. Biol. Lett. 2 (1996) 117–124.

[16] J.V. Beck, K.D. Cole, A. Haji-Sheikh, B. Litkouhi, Heat Conduction using Greens functions, Hemisphere Publ. Corp., Washinghton, 1992.

[17] C.W. Tittle, Boundary value problems in composite media: quasi orthogonal functions, J. Appl. Phys. 36 (4) (1965) 1486–1488.

[18] F. de Monte, Multi-layer transient heat conduction using transition time scales, Int. J. Thermal Sci. 45 (2006) 882–892.

[19] C. Hwang, D. Wu, E.R. Edelman, Physiological transport forces govern drug distribution for stent-based delivery, Circulation 104 (5) (2001) 600–605.